



LAWRENCE
LIVERMORE
NATIONAL
LABORATORY

LLNL-PROC-832404

Impact of divertor material on neutral recycling and discharge fueling

I. Bykov, D. L. Rudakov, A. Yu. Pigarov, E. M. Hollmann, J. Guterl, J. A. Boedo, C. P. Chrobak, T. Abrams, H. Y. Guo, C. J. Lasnier, A. G. McLean, H. Q. Wang, J. G. Watkins, D. M. Thomas

March 4, 2022

17th international conference on plasma-facing materials and
components for fusion applications
Eindhoven, Netherlands
May 20, 2019 through May 24, 2020

Disclaimer

This document was prepared as an account of work sponsored by an agency of the United States government. Neither the United States government nor Lawrence Livermore National Security, LLC, nor any of their employees makes any warranty, expressed or implied, or assumes any legal liability or responsibility for the accuracy, completeness, or usefulness of any information, apparatus, product, or process disclosed, or represents that its use would not infringe privately owned rights. Reference herein to any specific commercial product, process, or service by trade name, trademark, manufacturer, or otherwise does not necessarily constitute or imply its endorsement, recommendation, or favoring by the United States government or Lawrence Livermore National Security, LLC. The views and opinions of authors expressed herein do not necessarily state or reflect those of the United States government or Lawrence Livermore National Security, LLC, and shall not be used for advertising or product endorsement purposes.

Impact of divertor material on neutral recycling and discharge fueling

I. Bykov¹, D.L. Rudakov¹, A. Yu. Pigarov¹, E.M. Hollmann¹, J. Guterl², J.A. Boedo¹, C.P. Chrobak³, T. Abrams³, H.Y. Guo³, C.J. Lasnier⁴, A.G. McLean⁴, H.Q. Wang³, J.G. Watkins⁵, D.M. Thomas³

¹University of California San Diego, La Jolla, CA, 92093-0417, USA

²Oak Ridge Associated Universities, Oak Ridge, TN 37831-0117, USA

³General Atomics, San Diego, CA 92186-5608, USA

⁴Lawrence Livermore National Laboratory Livermore, CA, 94550, USA

⁵Sandia National Laboratory, Livermore, CA, 94551-0969, USA

E-mail: ibykov@ucsd.edu

Abstract

Experiments with the lower divertor of DIII-D during the Metal Rings Campaign (MRC) show that the fraction F of atomic D in the total recycling flux is material-dependent and varies through the ELM cycle, which may affect divertor fueling. Between ELMs, $F_C \sim 10\%$ and $F_W \sim 40\%$, consistent with expectations if all atomic recycling is due to reflections. During ELMs, F_C increases to 50% and F_W to 60%. In contrast, the total D recycling coefficient including atoms and molecules R stays close to unity near the strike point where the surface is saturated with D. During ELMs, R can deviate from unity, increasing during high energy ELM-ion deposition (net D release) and decreasing at the end of the ELM which leads to ability of the target to trap the ELM-deposited D. The increase of $R > 1$ in response to an increase in ion impact energy E_i has been studied with small divertor target samples using Divertor Materials Evaluation System (DiMES). An electrostatic bias was applied to DiMES to change E_i by 90 eV. On all studied materials including C, Mo, uncoated and W-coated TZM (>99% Mo, Ti, and Zr alloy), W, and W fuzz, an increase of E_i transiently increased the D yield (and R) by $\sim 10\%$. On C there was also an increase in the molecular D₂ yield, probably due to ion-induced D₂ desorption. Despite the measured increase in F on W compared to C, attached H-mode shots with OSP on W did not demonstrate a higher inter-ELM pedestal recovery rate and higher pedestal density. About 8% increase in the edge density could be seen only in L-mode scenarios. The difference can be explained by higher D trapping in the divertor and lower divertor fueling efficiency in H- vs. L-mode.

Keywords: DIII-D tokamak, tungsten, recycling, fueling

1. Introduction

The quest for materials suitable for plasma facing components (PFCs) of magnetic confinement fusion devices is driven by stringent requirements to their thermo-mechanical, chemical, and radiation properties: melting point, ductility, thermal diffusivity, physical and chemical erosion rates and maximum permissible concentration in the plasma, H diffusivity, ability to form bonds and co-deposit with H, and effects of high dose neutron irradiation. Still widely used for PFCs, graphite has a number of advantages including high thermal diffusivity, no melting, relatively low $Z_c=6$, which provides very forgiving operation of tokamaks with a graphite first wall. Nevertheless, because of high co-deposition rates with H and its radiation-induced embrittlement graphite has largely been discarded as a PFC material for burning plasma applications. The next generation

tokamak ITER as well as the largest present-day machine JET with ITER-Like Wall (JET-ILW [1]) have a similar combination of PFC materials: Be in the main chamber and W in the divertor. Several other machines like ASDEX-Upgrade (AUG [2]) have transitioned from full-C to fractional W divertor and wall coverage. Recycling on PFC surfaces constitutes a strong intrinsic source of neutral deuterium for plasma fueling. Therefore, a change to the PFC composition may be expected to affect the energy and the flux of the neutral D through the change of the particle and energy reflection coefficients.

It has been noted upon transition to JET-ILW that some properties of the H-mode pedestal and plasma performance have changed compared to JET-C due to the difference in the PFC materials. The pedestal degradation and the decrease of the ELM stability are associated with a larger relative shift between the pedestal n_e and T_e profiles and smaller

normalized pressure gradient in JET-ILW [3]. The effect of the material change was similar to an increase of the gas puff rate in JET-C [3]. A lower L-H transition power threshold seen in both JET-ILW and AUG was also associated with the materials change [4]. In contrast to JET-ILW and AUG, in DIII-D only a small fraction (0.6%) of the total wall area was replaced with W-covered inserts in a dedicated metal rings campaign in 2016. In this work we study the consequences of the material change in the divertor of DIII-D for the local neutral fuel sourcing and the edge profile modification.

2. Experimental approach

DIII-D is a full-C tokamak with major and minor radii of 1.67 and 0.67 m [5]. DIII-D has a versatile suite of edge and divertor diagnostics that are described in [6-8], including CO₂ interferometers, core and edge Thomson Scattering (TS), Charge Exchange Recombination Spectroscopy (CER), filtered photomultipliers (filterscopes), and filtered cameras. The shelf of the lower outer divertor is equipped with the Divertor Material Evaluation System (DiMES) [7], allowing exposure of material samples aligned with the divertor surface. DiMES can be used to study local recycling on circular 6 mm diameter samples made of different materials. An example of the DiMES head design is given in [8]. DiMES samples can be electrically biased to change the ion incidence energy E_i . In L-mode discharges biasing DiMES allowed the study of the recycling response to an E_i increase, similar to what happens during an ELM due to the initial high-energy ion component.

Simultaneous time and spatially resolved measurements of atomic (D) and molecular (D₂) deuterium recycling fluxes were made with absolutely calibrated split filtered imaging of the lower divertor using atomic D_α emission (656.5 nm) and molecular Fulcher-band (600-640 nm) emission. The time and spatial resolutions of these measurements are ~2 ms and 3 mm. General aspects of fast imaging on DIII-D is described in [9]. The split imaging was used to calculate the fraction of the atomic deuterium F_A in the recycling flux [10]:

$$F_A = \frac{\Gamma_A}{\Gamma_A + 2\Gamma_M} \simeq 1 - \frac{2}{\frac{\Phi(D_\alpha)S/XB(D_\alpha)}{\Phi(F)D/XB} + 1} \quad (1)$$

Γ_A and Γ_M are atomic and molecular deuterium recycling fluxes, Φ is the measured photon flux, S/XB [11] and D/XB [12] are inverse photon efficiencies with respect to D ionization and D₂ dissociation.

Any change in recycling properties of DiMES samples is local and therefore does not influence the global plasma performance. Such a study would require to replace a fraction of the PFC area with a toroidally symmetric array of components made of a different material. In June-July 2016, the lower divertor of DIII-D has been modified by inserting 2 toroidally continuous 5 cm wide W-covered TZM (an alloy with >99% of Mo) rings. The month-long mini campaign that followed was called the Metal Rings Campaign (MRC) [6].

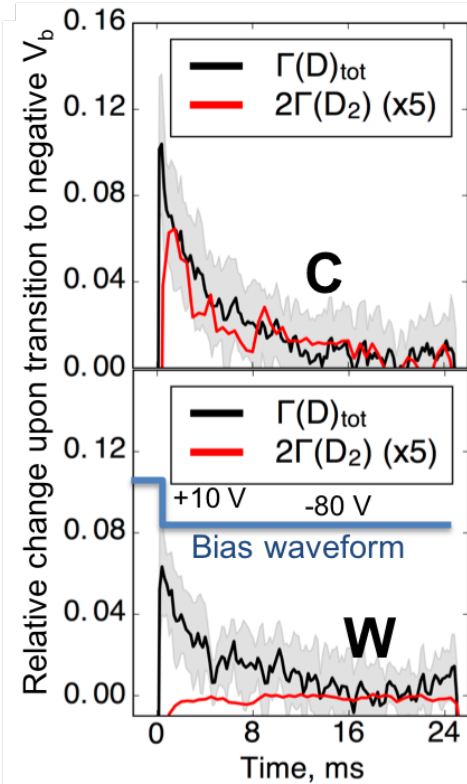


Fig. 1 Relative change of the total $\Gamma(D)_{tot} = \Gamma(D) + 2\Gamma(D_2)$ and molecular $2\Gamma(D_2)$ deuterium recycling fluxes on C and on W on DiMES in response to an E_i increase by 90 eV. The baseline signal is subtracted. Both materials show a similar ~10% increase in the total recycled D.

The main objective of MRC was to study W sourcing and transport in a low-Z environment. Our focus will be on the effect of adding W in the divertor on local recycling and its consequences for fueling and modification of midplane plasma profiles.

3. Results and discussion

Small-scale DiMES material tests

A set of metal samples including C, Mo, uncoated and W-coated TZM (>99% Mo), W, and W fuzz, were exposed on DiMES in a series of L-mode shots. A rectangular bias signal V_b consisting of +10 V and -80 V with respect to the ground was applied to DiMES in order to modulate the ion impact energy. Keeping V_b below the plasma potential makes the collected current I_b close to that of the ion saturation. This helps isolate the effect due to an increase in the ion energy E_i .

Fig. 1 shows the relative change of the total and molecular deuterium flux upon an increase of the ion incidence energy (E_i) due to a change in the applied bias. The plotted quantity is equivalent of $R-1$ for the total (atomic and molecular) and molecular deuterium, where R is the recycling coefficient. The time vector is centered at the time when V_b is switched from +10 V to -80 V, and the data is obtained by coherently

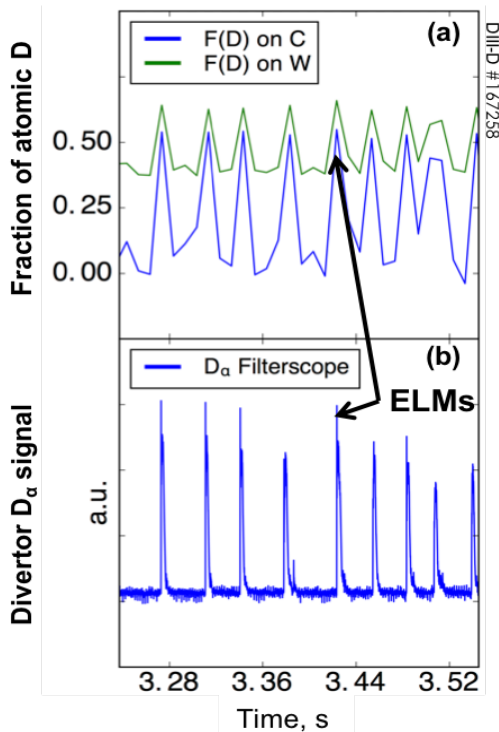


Fig. 2 Fraction of atomic D (a) sourced near OSP on C and on W during a 0.3 s window of an ELMMy H-mode shot during MRC, measured by fast split imaging of D_α and D_2 signal. Divertor filterscope D_α (b) is plotted to identify the ELMs.

averaging over ~ 10 V_b cycles. The increase of E_i by 90 eV from $E_i \approx 3T_e + 2T_i \approx 140$ eV to 230 eV leads to a transient increase of both the total neutral D flux and its molecular fraction on C. On W there is no increase of the D_2 component, therefore the increase of the total D is only due to atoms. On both C and W the surface D atomic concentration corresponding to the saturation of deuterium decreases with E_i . Therefore, surface becomes super-saturated with D when E_i suddenly increases, and the excess D is promptly released. About 20 ms after V_b changes, the recycling coefficient R stabilizes close to unity due to surface saturation.

The peak at $t=0$ is attributed to a depletion of the “surface reservoir” by more energetic D^+ ions and implies that, temporarily, $R>1$. A similar effect was probably seen on graphite saturated by D at implantation energy 1 keV when the beam energy was switched to 6 keV [13]. In a tokamak experiment a similar depletion of the surface D reservoir is probably what causes a short D_α spike when the limiter bias is turned on at -200 V, see Fig.1 in [14]. The ion induced detrapping of molecular D in saturated graphites has been explained and modelled by the recombination of beam-activated and trapped atomic D in the bulk within the implantation depth and its quick diffusion to the surface through micro cracks and pores [15]. This mechanism may be nonexistent in W which explains why there is no D_2 spike in response to E_i increase on W. The D peak on both W and C is probably due to direct sputtering of the saturated surface

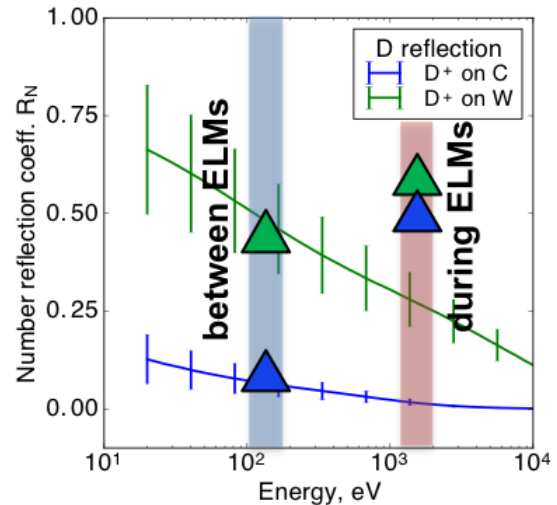


Fig. 3 Calculated D number reflection coefficient R_N as function of D normal incidence energy (lines) and measured in MRC H-mode shot 167258, Fig. B(a), fraction of D recycled in atomic form, between and during ELMs on C and on W (triangles).

D layer. Other studied metals behaved qualitatively similar to W.

In ELMMy H-modes in tokamaks the regimes with $R>1$ were anticipated during ELMs due to depletion of the surface reservoir [16]. The transiently released D has low energy and does not contribute to the edge fueling but it increases the local plasma density, which may lead to the transient higher recycling regime [17] or even detachment after an ELM. On C this can be aided by the higher fraction of molecules in the recycling flux that can contribute to the power and momentum dissipation and can help achieve detachment through molecule assisted recombination (MAR) [18]. Shortly after the ELM crash, both the D expelled from the pedestal and the D released from the target are re-absorbed by the divertor/wall material.

The slow desorption of D_2 between ELMs supplies fuel for pedestal recovery. D_2 desorbs at about the wall temperature, and Frank-Condon D atoms due to D_2 dissociation have energy of the order of 2 eV and are ionized in the scrape off layer (SOL), without reaching the separatrix. In order to gain sufficient energy to cross the separatrix, the low-energy deuterium due to desorption has to either undergo a charge-exchange collision with an edge ion or become ionized and reflect from the divertor target. This is why the inter-ELM reflection properties of the divertor material become important. Therefore, the two material-related quantities responsible for fueling are the energy and the reflection

coefficients. Both are higher on W than on C; therefore, one expects more efficient divertor fueling with W in the divertor.

Large scale W-divertor experiment during MRC

During MRC, the split imaging of the lower divertor was performed while keeping the W Ring within the view. The fractions of recycled atoms FC and FW were calculated using Eq. (1) for a Type-I ELM My H-mode shot with attached outer strike point (OSP), Fig. 2(a). The data is averaged over 2 ms camera integration windows. ELMs are identified by the spikes in the fast divertor $D\alpha$ signal from filterscopes, Fig.2(b). FW and FC averaged over many ELM cycles are plotted by triangles in Fig. 3. The inter-ELM data for both materials are close to the values suggested by a simple reflection model (solid lines) [19] if the D^+ incidence energy is calculated as $E_i \approx 3T_e + 2T_i \approx 150$ eV, similar to the L-mode case, using the Langmuir Probe (LP) Te measurements and assuming $T_e \approx T_i$. This suggests that if the recycling coefficient between ELMs is $R \approx 1$, then the atomic fraction of recycled D is mostly due to reflections. The low values for FC are in agreement with, the old H-mode data from JET-C, see Fig. 7 in [10]. During ELMs the measured F increased on both W and C. This contradicts the model expectation of lower D reflection probability at higher E_i (assuming $E_i \approx 2$ keV ~ 4.2 times pedestal Te during the initial ELM phase [20]). This may be indicative of the key role that other atom release processes play during ELMs, for example, ion-induced desorption and D sputtering, see Fig.1 in [10] and references therein. The fraction of atoms from the surface could increase if the surface temperature T_{surf} increases above ~ 1100 K, see Fig. 11 in [12], but in DIII-D T_{surf} is usually much lower even during ELMs.

In order to assess the effect of the OSP material change on the midplane D^+ density n_{D^+} during the MRC, we compare the edge profiles in discharges with the OSP on C and on W. The changes to the equilibrium are kept minimal and only the X-point is shifted inward by ~ 5 cm, Fig. 4(a). n_e profiles are measured by the core and edge TS and mapped onto the normalized poloidal flux coordinate ψ_n . The density profiles of C^{6+} are measured with CER. The D^+ density is calculated as $n_D = n_e - 6 \cdot n_{C^{6+}}$; this is accurate inside the separatrix and in the near SOL in the main chamber, where C, the main impurity ion in DIII-D, is fully ionized.

Despite the measured difference in the OSP recycling in attached H-mode shots, there was no significant difference in inter-ELM n_{D^+} profiles when OSP was placed on C and on W, Fig.4(b). This suggests that the fueling rate through the outer divertor was inefficient, probably due to trapping of D near the strike point. In attached L-modes, in contrast, there was a noticeable 8% increase of the edge density when OSP was placed on W, Fig.4(c), qualitatively similar to the n_e density increase in L-mode seen on ASDEX Upgrade (AUG) upon transition from C to W PFCs. Adding gas puff to detach

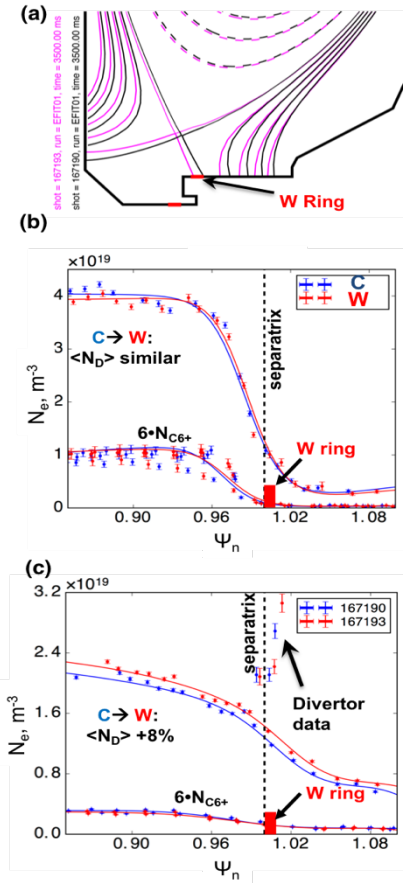


Fig. 4 (a) Change of the divertor equilibrium in order to move OSP from C to the inboard side of the W Ring. In H-mode (b) there is no significant change of the edge n_e when OSP is moved from C to W, while in L-mode (c) there is an 8% increase in the edge n_e . The $N_{C^{6+}}$ profiles in (b, c) show that there is no change in impurity profiles in both L- and H-modes in response to the OSP shift on W. Solid lines show polynomial fit to the data.

the divertor in AUG removed the difference in the profiles, which supports the important role of W in the divertor for fueling in attached conditions [21]. Unlike DIII-D, AUG also observed an increase in n_e between ELMs in attached H-modes which may be due to the fact that AUG had a larger area of the divertor and the main chamber covered in W.

The recycling response of a saturated PFC surface to an ELM can therefore be divided into four phases:

(i) During the initial ELM crash $R > 1$ and the surface D reservoir gets depleted. Here we neglect the surface temperature T_{surf} effect on the D thermal diffusivity because in DIII-D a single ELM only leads to temporary increase of T_s by a few 10 °C;

(ii) The D brought by the ELM recycles at the target and adds to the neutral D and plasma density increase near the target. In addition, the high energy D^+ population cools down as the energy recycling is much less efficient than the particle recycling;

(iii) The surface saturates with D. The extra D brought by the ELM gets implanted and co-deposited farther away from the strike point;

(iv) Between ELMs D is slowly released at ~ 20 T-L/s from the wall. Along with other sources (gas puffing and neutral beam injection), this release provides pedestal density recovery. Shifting the wall gas balance and reducing effective R could lead to lower n_e recovery rates between ELMs and lower ELM frequency. This may be realized by in-situ wall conditioning [22]. Contrariwise, running with heated PFCs can increase the rate of thermal desorption and increase the recovery rate and the ELM frequency.

4. Summary

The ELM response of fuel recycling in the form of atoms and molecules has been studied in the divertor of DIII-D on biased DiMES samples and on W divertor inserts during the MRC. On DiMES an increase of the ion incidence energy E_i by 90 eV triggered a temporary increase of recycling of less than $\sim 10\%$. On all studied metals that increase was due to atomic D, whereas on C the increase was also due to ion-induced molecular D2 re-emission. This effect is likely even stronger during ELMs, which add in excess of 1 keV to the inter-ELM ion energy. In an H-mode discharge with Type-I ELMs the inter-ELM atomic D recycling was due to reflections but during ELMs the atomic fraction F increased despite the expectations. This suggests that during ELMs D sources other than prompt reflection become important. The increase of the number and the energy of the reflected D atoms on W as compared to C may lead to more efficient divertor fueling with the OSP on W.

This hypothesis was tested during the MRC, where W under the outer strike point has led to an 8% increase of the midplane density in L-mode scenarios. This is attributed to the deeper penetration and higher flux of fast reflected D on W compared to C. During H-modes, the midplane profiles were not affected, probably because of higher trapping of D in the divertor and lower contribution of divertor neutrals to the edge fueling.

Even though a change of the PFC material from full-C to W and Be (JET-ILW) or full-W (AUG) performed in medium scale present day machines impacted the mid plane plasma profiles, in ITER the opacity of the SOL for neutrals will make the role of the wall less important. Divertor detachment will inhibit the prompt high-energy D⁺ reflection source. Therefore, in the divertor of ITER, the main effect of W on plasma conditions may be in controlling the detachment by setting the source of D2 molecules. Due to the transport of Be eroded in the main chamber, a deposited layer will grow on W in net deposition zones and a mixed Be-W layer form in erosion zones [23]. This could reduce the effective mass number of the surface material and reduce the energy and the

fraction of fast reflected D, bringing the conditions closer to those in low-Z PFC machines.

Acknowledgements

This material is based upon work supported by the U.S. Department of Energy, Office of Science, Office of Fusion Energy Sciences, using the DIII-D National Fusion Facility, a DOE Office of Science user facility, under Awards ¹DE-FG02-07ER54917, ²DE-AC05-06OR23100, ³DE-FC02-04ER54698, ⁴DE-AC52-07NA27344, ⁵DE-NA0003525.

Disclaimer: This report was prepared as an account of work sponsored by an agency of the United States Government. Neither the United States Government nor any agency thereof, nor any of their employees, makes any warranty, express or implied, or assumes any legal liability or responsibility for the accuracy, completeness, or usefulness of any information, apparatus, product, or process disclosed, or represents that its use would not infringe privately owned rights. Reference herein to any specific commercial product, process, or service by trade name, trademark, manufacturer, or otherwise does not necessarily constitute or imply its endorsement, recommendation, or favoring by the United States Government or any agency thereof. The views and opinions of authors expressed herein do not necessarily state or reflect those of the United States Government or any agency thereof.

References:

- [1] Romanelli F., et al., *Nucl. Fusion*, 53(2013)104002
- [2] Neu R., Kallenbach A., Balden M., et al., *J. Nucl. Mater.*, 438(2013)S34-S41
- [3] Stefanikova E. et al., *Nucl. Fusion* 58(2018)056010
- [4] Wolfrum E. et al., *Nucl. Mater. Energy* 12(2017)18-27
- [5] Luxon J. L. 2002 *Nucl. Fusion* 42 614
- [6] Bykov I. et al., *Phys. Scripta*, 2017, T170
- [7] Rudakov D.L. et al., 2017 *Fusion Eng. Design.*, 124, 196
- [8] Bykov I. et al., *Nucl. Mater. Energy*, 12(2017)379-385
- [9] R.A. Moyer, et al., *Rev. Sci. Instr.*, 89, 10E106(2018)
- [10] Pospieszczyk A. et al., *J. Nucl. Mater.*, 337-339(2005)500-504
- [11] Summers, H. P. (2004) The ADAS User Manual, version 2.6 <http://www.adas.ac.uk>
- [12] Mertens Ph. et al., *Plasma Phys. Control. Fusion*, 43(2001)A349-A373
- [13] B.M.U. Scherezer, J. Wang, and W. Möller, *J. Nuclear Mater.* 176&177(1990)208-212
- [14] P. Couturie et al., *J. Nucl. Mater.*, 176&177(1990)825-829
- [15] K. Morita and Y. Hasebe, *J. Nucl. Mater.*, 176&177(1990)825-829
- [16] S. Wiesen et al., *Nucl. Fusion* 57(2017)066024
- [17] T. Abrams et al., *Nucl. Mater. Energy*, 17(2018)164-173

- [18] E.M. Hollmann, *et al.*, *Plasma Phys. Control. Fusion*, 48(8)1165, 2006
- [19] Thomas E.W., Janev R.K., and Smith J.J., “Particle Reflection from Surfaces – a Recommended Data Base”, IAEA Nuclear Data Section, 96p.
- [20] Guillemaut C. *et al.*, *Phys. Scr.*, T167(2016)014005
- [21] T. Lunt, F. Reimold, E. Wolfrum, D. Carralero, Y. Feng, K. Schmid, and the ASDEX Upgrade Team, *Plasma Phys. Control. Fusion*, 59(2017)055016
- [22] Bortolon A., *Nucl. Mater. Energy*, 19(2019)384-389
- [23] Schmid K., *Nucl. Fusion*, 48(2008)105004